Environmental Applications

New Developments and Challenges in Remote Sensing, Oluić Z. Bochenek (ed.)
©2007 Millpress, Rotterdam, ISBN 978-90-5966-053-3

Qualitative distinction between terrain deformations and processing errors, and quantitative description of deformations for the 3-pass interferometry

M. Borik
Faculty of Civil Engineering, Czech Technical University, Prague, Department of Mathematics

I. Capkova, L. Halounova & J. Kianicka
Faculty of Civil Engineering, Czech Technical University, Prague, Department of Mapping and Cartography

Keywords: 3-pass differential interferometry, deformation monitoring, differential interferogram, subsidences, phase, coherence

ABSTRACT: The 3-pass interferometry means that we use three scenes where one pair (topo pair) is considered to have no influence on a deformation. The DEM is already derived in radar coordinates from this pair, and consequently this influence is also subtracted from deformation pair (deformation pair). The topo interferogram must be unwrapped first and then rewrapped in order to have the same height ambiguity as the deformation interferogram. This method is used to remove the topographically induced phase from the interferogram containing topography, deformation and atmosphere. The perpendicular baseline of the topo pair should be longer than that of the deformation pair to prevent that noise is multiplied. The advantage of the 3-pass interferometry is the fact that the whole processing is performed in the master slant range coordinate system and only the coregistration of complex SAR images is necessary. Both pairs (topo and deformation pair) have the same master scene.

When used for deformation mapping, the perpendicular baseline should be as short as possible in order to reduce the topographic signal in the interferogram as much as possible. The temporal baseline should be long enough to allow the deformations to occur, but the deformations cannot be too large. If the deformation slope exceeds 2.8 cm, phase unwrapping is very unreliable, and these deformations also cause decorrelation, especially when occurring in the azimuth direction. There are many spots (patches) in an interferogram which need to be verified in other interferograms. In this paper, we take two cases of topo pair into account. We changed master and slave scenes in the topo pair, and obtained two results for the phase of the differential interferogram. Then we can compare both phases and make conclusions if an expected subsidence or landslide occurs there.

1 INTRODUCTION

For topographic or deformation monitoring, data selection is often performed with the purpose to eliminate rain and snow. If there is no storm (or similar phenomenon) in the mapped area, the atmospheric influence usually has a long-wave characteristic, i.e. it changes slowly in the area (Hanssen 2001). Orbit errors and atmospheric

influence should be reduced together, establishing fictive satellite positions which are obtained by minimizing the number of residual fringes in the interferogram. If we use fictive satellite positions, artifacts are corrected at four corners of the image so the worst artifact occurs close to the center of the image (Tarayre & Massonnet 1994). However, we used a different method – empirical one – calculating number of fringes, and they are removed.

2 CHOICE OF THREE SCENES FOR THE 3-PASS INTERFEROMETRY

For choice of 3 scenes, we used the following criteria: the interferometric pair is chosen only from winter time, from December 1 until April 10 in the 1998–2004 period. The perpendicular baseline of the deformation pair is as small as possible (smaller than 100 m). We need to observe an area with high probability of terrain deformations. This area was found in the Northern Bohemia Brown Coal Basin in vicinity of 2 cities – Teplice and Usti nad Labem. The mining had been finished, but we can study after-reclamation activities nowadays. And the last condition was that there should be no precipitations during the acquisition and three days before, and no snow cover as well in this time. Using these criteria, 3 acquisition dates and satellites from two tracks were chosen: December 28, 1998 (ERS-2), March 7, 1999 (ERS-1) and March 8, 1999 (ERS-2). Two cases of topo pair were processed. March 8 was used as a master scene and March 7 as a slave scene in case A. March 7 as a master and March 8 as a slave in case B. The acquisition date – December 28 – always created the deformation pair with the master scene. The temporal baseline of deformation pair is negative.

Perpendicular baseline of the topo pair is 107 m. This baseline for the deformation pair in case A is 96 m and that for deformation pair in case B is 16 m.

3 METHOD

3.1 *Relationship between the phase of the differential interferogram and the occurred deformation*

Deformation phase $\Phi_{\Delta\rho}$ corresponds to the deformation occurred Δr (Kampes 1999):

$$\Phi_{\Delta r} = -\frac{4\pi}{\lambda}\Delta r. \tag{1}$$

The phase of the differential interferogram depends on baselines of both pairs. Both baselines are not constant throughout the image and therefore the phase of the differential interferogram can change as well.

In cases A and B, the temporal baseline of deformation pair is negative. Therefore, it follows from (1) that

$$\Delta r = \frac{\lambda}{4\pi}\Phi_{\Delta r}. \tag{2}$$

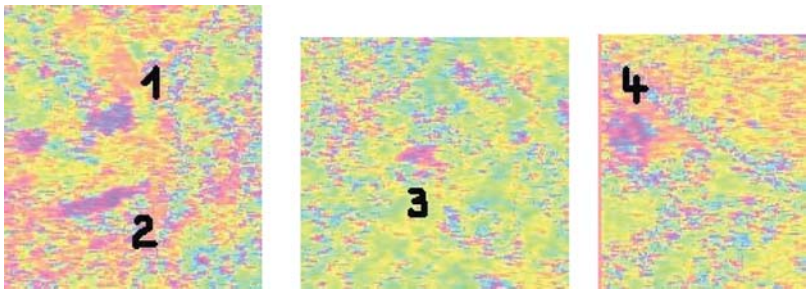

Figure 1–3. Differential interferogram with 4 suspected areas of subsidence.

It means that phases of the differential interferogram are concave in geographical terminology (in case of subsidences).

Another important feature of this method is that all measurements are relative. Theoretically, the phase of the differential interferogram should be zero in the areas of no deformation, but there are systematic errors influencing the measurements and therefore the deformations can be determined only relatively with respect to their vicinity. According to (2), we can determine expected deformations quantitatively.

3.2 *Processing*

Places suspected from deformations were extracted in rectangle shapes. Colored points from Fig. 1A–4B in Appendix are values of phases in pixel/line directions in these rectangles. Different colors denote different pixels/lines. Figures 1–3 represent areas 1–4. March 8 as a master and March 7 as a slave in the A case, and March 7 as a master and March 8 as a slave for the B case. Colored points with individual symbols denote 1 pixel/line and these values were adjusted by polynomials of the sixth order (dashed curves). Final values of deformations were derived from curves between two horizontal tangents (upper and lower) according to equation (2).

Both cases A and B were performed independently from each other, since they have two different perpendicular baselines of two deformation pairs, two different topo pairs where master images were not the same, and two different coregistration polynomial as well. That polynomial was calculated for different tie points.

Coherence has to be taken into account. Clearly visible ‘‘deformations’’ in differential interferogram can be easily confused with agriculture areas. However, there can be no subsidences and landslides here, only small changes in terrain heights as a consequence of agricultural cultivation. Terrain could have thin ice layer as well.

4 RESULTS

Theoretically, the phase of the differential interferogram should be zero in areas of no deformation, but there are systematic processing errors influencing the measurements and therefore the deformations can be determined only relatively with respect to their vicinity.

It can be seen in figures that phase of the differential interferogram is in $[-\pi, \pi)$, and thus the phase ambiguity occurs. Therefore we are not able to recognize deformations higher than 2.8 cm in 1 pixel. For subsidence confirmation, we demand as continuous phase as possible with a sufficient number of neighboring pixels and lines (at least 5 pixels/lines). Each point in Fig. 1A–4B denotes pixel phase of original pixel size (4.5×20 m). The phase of the differential interferogram was not "unwrapped". To get reliable results concerning subsidences, and to compare case A and case B, parts of figures (in red rectangles) were copied up or down for about 1 fringe (i.e. 2.8 cm or 2π) see Fig. 1B, 2B, 3B, 4A, 4B. The shift was necessary to perform for the smaller baseline (16 m).

Spots in differential interferograms were verified by means of both cases A and B. Two results were obtained for the phase of the differential interferogram and confirmed existence of subsidences.

There are 4 suspected areas of subsidence in Fig. 1–3. To determine potential terrain deformations, the suspected areas of subsidence must be sufficiently coherent. Incoherent areas can be regarded as a "loss" of data, as areas with decorrelation even though they can comprise deformations.

Every the numbered area in Fig. 1–3 has a very good coherence. Therefore we are able to denote expected subsidences. One area in Fig. 1 (on the left side) was not chosen because this area is not sufficiently coherent. Deformations can be seen in Fig. 1A–4B in the Appendix. Subsidence of the first area is 1.5 cm, area 2 subsided for about 1.1 cm. The third area has 1.3 cm subsidence and subsidence of the fourth area is 1.2 cm. All subsidences and their particular values are depicted for cases A and B.

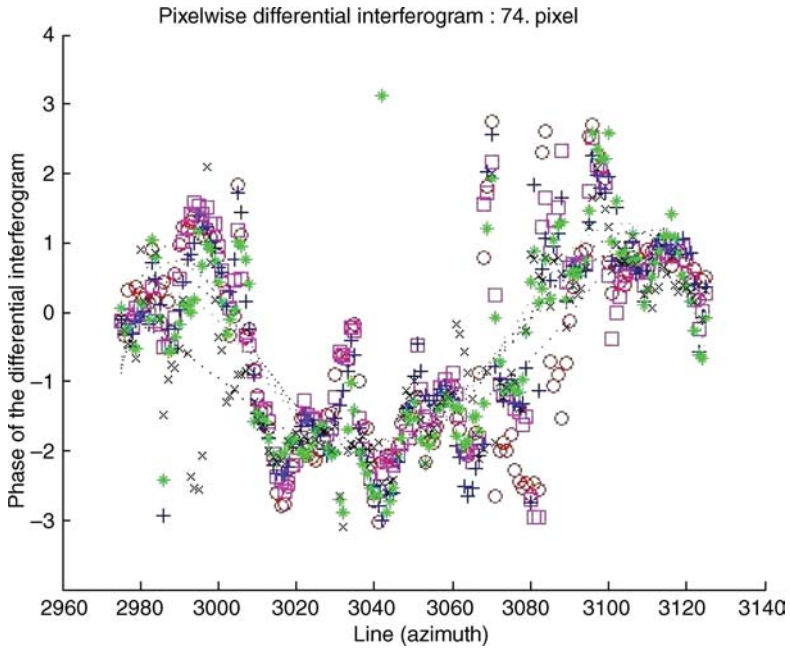

Figure 1A. Differential interferogram (case A, area 1) where vertical axis is the phase of the differential interferogram (in radians).

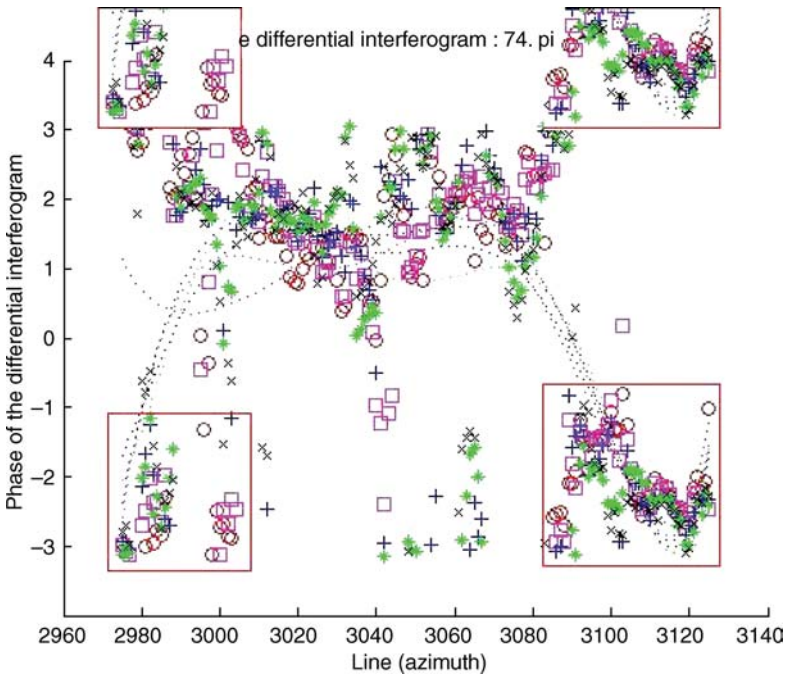

Figure 1B. Differential interferogram (case A, area 1) where vertical axis is phase of the differential interferogram (in radians).

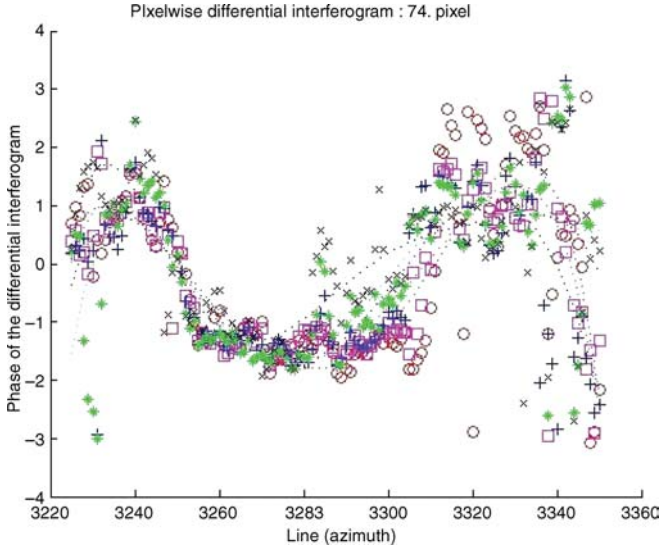

Figure 2A. Differential interferogram (case A, area 1) where vertical axis is phase of the differential interferogram (in radians).

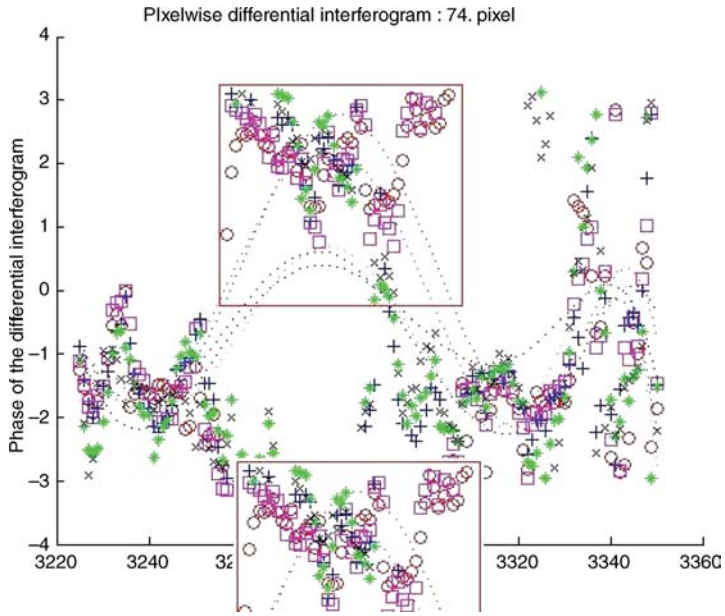

Figure 2B. Differential interferogram (case A, area 1) where vertical axis is phase of the differential interferogram (in radians).

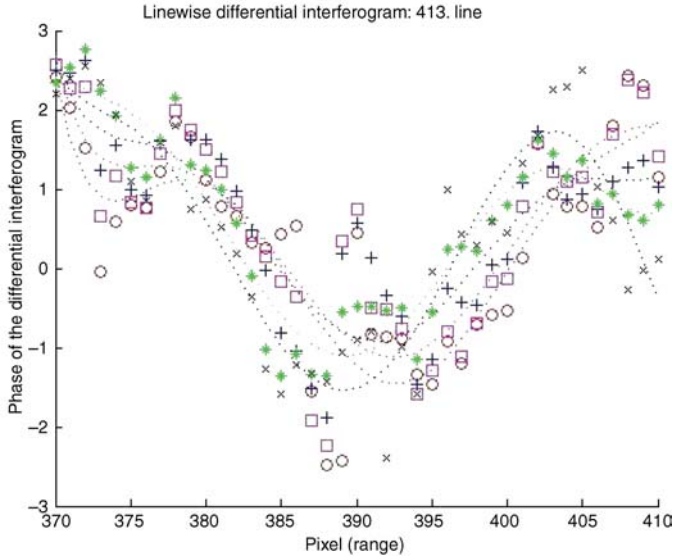

Figure 3A. Differential interferogram (case A, area 1) where vertical axis is phase of the differential interferogram (in radians).

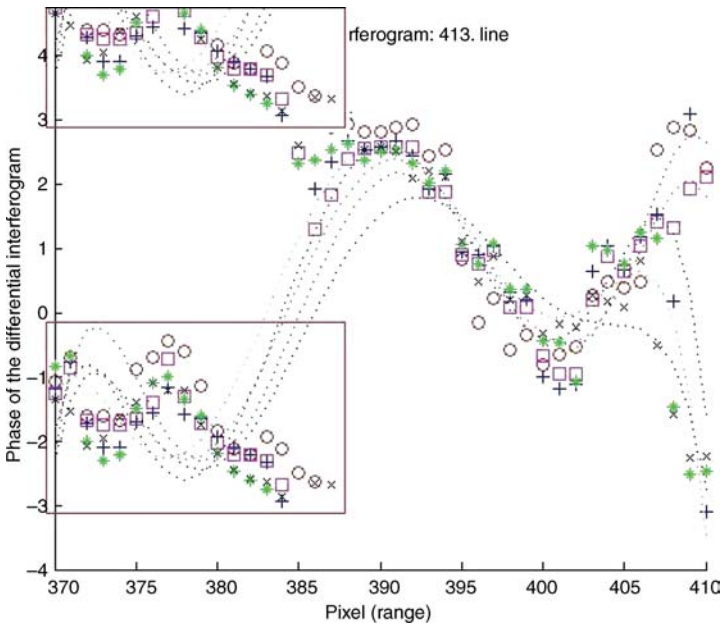

Figure 3B. Differential interferogram (case A, area 1) where vertical axis is phase of the differential interferogram (in radians).

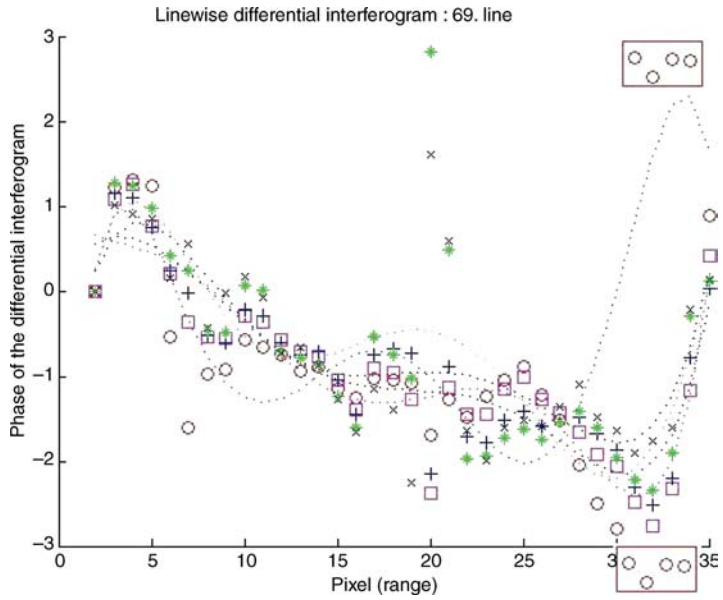

Figure 4A. Differential interferogram (case A, area 1) where vertical axis is phase of the differential interferogram (in radians).

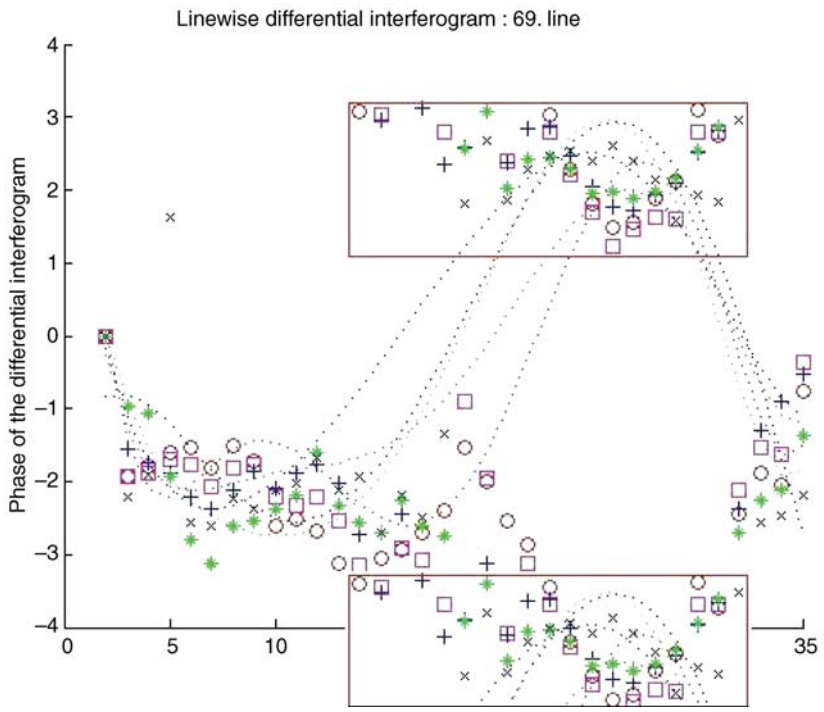

Figure 4B. Differential interferogram (case A, area 1) where vertical axis is phase of the differential interferogram (in radians).

5 CONCLUSION

3-pass interferometry using 2 different topo pairs, two 2 different deformation pairs and different polynomial functions for coregistration evaluated independently in pixel/line directions from differential interferograms yields the same results of both cases A and B of deformations.

Adjustment of these values denoted deformations in four small undermined areas. The calculated values of phases adjusted by regression curves are two-fold. The first group shows all values alongside the curves. The second group is different. One part of the values is alongside the curves and the other one shifted for 2π phase represent the case where one phase of the differential interferogram approaches $+\pi$ and the other $-\pi$ creating nearly 2π difference and the trend of points should have continuously changing derivative.

The necessity of adjustment is a result of errors whose exact correction is still unknown.

ACKNOWLEDGEMENT

This paper was supported by GA CZ grant No. GA 205/03/D155.
Data were granted by ESA in the framework of Category 1 projec: Interferometry used for landslide and land subsidence detection in the undermined area and in the area with abandoned open brown coal mines.

REFERENCES

Hanssen, R.F. 2001. Radar Interferometry: Data Interpretation and Error Analysis. *Kluwer Academic Publishers*, Dordrecht.

Kampes, B. 1999. Delft Object-Oriented Radar Interferometric Software: Users manual and Technical Documentation. Delft University of Technology, Delft.

Tarayre, H. & Massonnet, D. 1994. Effects of refractive atmosphere on interferometric processing. *Igarss94*, 717–719.